Computational Methods in Applied Sciences

Manolis Papadrakakis
Michalis Fragiadakis
Nikos D. Lagaros *Editors*

Computational Methods in Earthquake Engineering

ECCOMAS
European Community on Computational Methods in Applied Sciences

Springer

Computational Methods in Earthquake Engineering

Computational Methods in Applied Sciences

Volume 21

Series Editor

E. Oñate
International Center for Numerical Methods in Engineering (CIMNE)
Technical University of Catalunya (UPC)
Edificio C-1, Campus Norte UPC
Gran Capitán, s/n
08034 Barcelona, Spain
onate@cimne.upc.edu
www.cimne.com

For other titles published in this series, go to
www.springer.com/series/6899

Manolis Papadrakakis • Michalis Fragiadakis
Nikos D. Lagaros
Editors

Computational Methods in Earthquake Engineering

Springer

Editors
Manolis Papadrakakis
National Technical Univ. Athens
Inst. Structural Analysis &
Seismic Research
Iroon Polytechniou Str. 9
157 80 Athens
Greece
mpapadra@central.ntua.gr

Nikos D. Lagaros
National Technical Univ. Athens
Inst. Structural Analysis &
Seismic Research
Iroon Polytechniou Str. 9
157 80 Athens
Greece
nlagaros@central.ntua.gr

Michalis Fragiadakis
National Technical Univ. Athens
Inst. Structural Analysis &
Seismic Research
Iroon Polytechniou Str. 9
157 80 Athens
Greece
mfrag@mail.ntua.gr

ISSN 1871-3033
ISBN 978-94-007-0052-9 e-ISBN 978-94-007-0053-6
DOI 10.1007/978-94-007-0053-6
Springer Dordrecht Heidelberg London New York

Cover design: SPi Publisher Services

Printed on acid-free paper

Springer is part of Springer Science+Business Media (www.springer.com)

Preface

The book provides an insight on advanced methods and concepts for design and analysis of structures against earthquake loading. It consists of 25 chapters covering a wide range of timely issues in Earthquake Engineering. The goal of this Volume is to establish a common ground of understanding between the communities of Earth Sciences and Computational Mechanics towards mitigating future seismic losses. Due to the great social and economic consequences of earthquakes, the topic is of great scientific interest and is expected to be of valuable help to the large number of scientists and practicing engineers currently working in the field. The chapters of this Volume are extended versions of selected papers presented at the COMPDYN 2009 conference, held in the island of Rhodes, Greece, under the auspices of the European Community on Computational Methods in Applied Sciences (ECOMASS).

In the introductory chapter of Lignos et al. the topic of collapse assessment of structures is discussed. The chapter presents the analytical modeling of component behaviour and structure response from the early inelastic to lateral displacements at which a structure becomes dynamically unstable. A component model that captures the important deterioration modes, typically observed in steel members, is calibrated using data from tests of scale-models of a moment-resisting connection. This connection is used for the two-scale model of a modern four-story steel moment frame and the assessment of its collapse capacity through analysis.

The work of Adam and Jäger deals with the seismic induced global collapse of multi-story frame structures with non-deteriorating material properties, which are vulnerable to the P–Δ effect. The initial assessment of the structural vulnerability to P–Δ effects is based on pushover analyses. More information about the collapse capacity is obtained with the Incremental Dynamic Analyses using a set of recorded ground motions. In a simplified approach equivalent single-degree-of-freedom systems and collapse spectra are utilized to predict the seismic collapse capacity of the structures.

Sextos et al. focus on selection procedures for real records based on the Eurocode 8 (EC8) provisions. Different input sets comprising seven pairs of records (horizontal components only) from Europe, Middle-East and the US were formed in compliance with EC8 guidelines. The chapter deals with the study of the RC bridges of the Egnatia highway system and also with a multi-storey RC building that was damaged during the 2003 Lefkada (Greece) earthquake. More specifically,

the bridge was studied using alternative models and accounting for the dynamic interaction of the deck-abutment-backfill-embankment system as well as of the superstructure-foundation-subsoil system. The building was studied in both the elastic and inelastic range taking into consideration material nonlinearity as well as the surrounding soil. The results permit quantification of the intra-set scatter of the seismic response for both types of structures, thus highlighting the current limitations of the EC8 guidelines. Specific recommendations are provided in order to eliminate the dispersion observed in the elastic and the inelastic response though appropriate modifications of the EC8 selection parameters.

Assimaki et al. study how the selection of the site response model affects the ground motion predictions of seismological models, and how the synthetic motion site response variability propagates to the structural performance estimation. For this purpose, the ground motion synthetics are computed for six earthquake scenarios of a strike-slip fault rupture, and the ground surface response is estimated for 24 typical soil profiles in Southern California. Next, a series of bilinear single-degree-of-freedom oscillators is subjected to the ground motions computed using the alternative soil models and the consequent variability in the structural response is evaluated. The results show high bias and uncertainty in the prediction of the inelastic displacement ratio, when predicted using the linear site response model for periods close to the fundamental period of the soil profile.

The chapter of Kappos et al. addresses the issue of pushover analysis of bridges sensitive to torsion, using as case-study a bridge whose fundamental mode is purely torsional. Parametric analyses were performed involving consideration of foundation compliance, and various scenarios of accidental eccentricity that would trigger the torsional mode. An alternative pushover curve in terms of abutment shear versus deck maximum displacement (that occurs at the abutment) was found to be a meaningful measure of the overall inelastic response of the bridge. It is concluded that for bridges with a fundamental torsional mode, the assessment of their seismic response relies on a number of justified important decisions that have to be made regarding: the selection and the reliable application of the analysis method, the estimation of foundation and abutment stiffnesses, and the appropriate numerical simulation of the pertinent failure mechanism of the elastomeric bearings.

Pardalopoulos and Pantazopoulou investigate the spatial characteristics of a structure's deformed shape at maximum response in order to establish deformation demands in the context of displacement-based seismic assessment or redesign of existing constructions. It is shown that the vibration shape may serve as a diagnostic tool of global structural inadequacies as it identifies the tendency for interstorey drift localization and twisting due to mass or stiffness eccentricity. This chapter investigates the spatial displaced shape envelope and its relationship to the three-dimensional distribution of peak drift demand in reinforced concrete buildings with and without irregularities in plan and in height. A methodology for the seismic assessment of rotationally sensitive structures is established and tested through correlation with numerical results obtained from detailed time history simulations.

The chapter of Cotsovos and Kotsovos summarises the fundamental properties of concrete behaviour which underlie the formulation of an engineering finite element

model that is capable to realistically predict the behaviour of (plain or reinforced) concrete structural forms for a wide range of problems from static to impact loading, bypassing the problem of re-calibration. The already published evidence that support the proposed formulation is complemented by four typical case-studies. For each case-study, the numerical predictions are computed against experimental data revealing good agreement.

The chapter of Wijesundara et al. investigates the local seismic performances of fully restrained gusset plate connections through detailed finite element models of a single storey single-bay frame that is located at the ground floor of the four storey frame. The chapter presents a design procedure, proposing an alternative clearance rule for the accommodation of brace rotation. Local performances of FE models are compared in terms of strain concentrations at the beams, the columns and the gusset plates.

Vielma et al. propose a new seismic damage index and the corresponding damage thresholds. The seismic behavior of a set of regular reinforced concrete buildings designed according to the EC-2/EC-8 prescriptions for a high seismic hazard level are studied using the proposed damage index. Fragility curves and damage probability matrices corresponding to the performance point are then calculated. The obtained results show that the collapse damage state is not reached in the buildings designed according the prescriptions of EC-2/EC-8 and that the damage does not exceed the irreparable damage limit-state for the buildings studied.

The application of discrete element models based on rigid block formulations to the analysis of masonry walls under horizontal out-of-plane loading is discussed in the chapter of Lemos et al. The problems raised by the representation of an irregular fabric as a simplified block pattern are addressed. Two procedures for creating irregular block systems are presented. One using Voronoi polygons and another based on a bed and cross joint structure with random deviations. A test problem provides a comparison of various regular and random block patterns, showing their influence on the failure loads.

Papaloizou and Komodromos discus the computational methods appropriate for simulating the dynamic behaviour and the seismic response of ancient monuments, such as classical columns and colonnades. Understanding the behaviour and response of historic structures during strong earthquakes is useful for the assessment of conservation and rehabilitation proposals for such structures. Their seismic behaviour involves complicated rocking and sliding phenomena that very rarely appear in modern structures. The discrete element method (DEM) is utilized to investigate the response of ancient multi-drum columns and colonnades during harmonic and earthquake excitations by simulating the individual rock blocks as distinct rigid bodies.

The study on the seismic behaviour of the walls of the Cella of Parthenon when subjected to seismic loading is presented in the chapter of Psycharis et al.. Given that commonly used numerical codes for masonry structures or drum-columns are unable to handle the discontinuous behaviour of ancient monuments, the authors adopt the discrete element method (DEM). The numerical models represent in detail the actual construction of the monument and are subjected to the three components

of four seismic events recorded in Greece. Time domain analyses were performed in 3D, considering the non-linear behaviour at the joints. Conclusions are drawn based on the maximum displacements induced to the structure during the ground excitation and the residual deformation at the end of the seismic motion.

The chapter of Dolsek studies the effect of both aleatory and epistemic (modelling) uncertainties on reinforced concrete structures. The Incremental Dynamic Analysis (IDA) method, which can be used to calculate the record-to-record variability, is extended with a set of structural models by utilizing the Latin Hypercube Sampling (LHS) to account for the modelling uncertainties. The results showed that the modelling uncertainties can reduce the spectral acceleration capacity and significantly increase its dispersion.

The chapter of Taflanidis discusses the problem of the efficient design of additional dampers, to operate in tandem with the isolation system. One of the main challenges of such applications has been the explicit consideration of the nonlinear behavior of the isolators or the dampers in the design process. Another challenge has been the efficient control of the dynamic response under near-field ground motions. In this chapter, a framework that addresses both these challenges is discussed. The design objective is defined as the maximization of the structural reliability. A simulation-based approach is implemented to evaluate the stochastic performance and an efficient framework is proposed for performing the associated design optimization and for selecting values of the controllable damper parameters that optimize the system reliability.

Mitsopoulou et al. study a robust control system for smart beams. First the structural uncertainties of basic physical parameters are considered in the model of a composite beam with piezoelectric sensors and actuators subjected to wind-type loading. The control mechanism is introduced and designed to keep the beam in equilibrium in the event of external wind disturbances and in the presence of mode inaccuracies using the available measurement and control under limits.

Panagiotopoulos et al. examine through simple examples the performance and the characteristics of a methodology previously proposed by the authors on a variationally-consistent way for the incorporation of time-dependent boundary conditions in problems of elastodynamics. More specifically, an integral formulation of the elastodynamic problem serves as basis for enforcing the corresponding constraints, which are imposed via the consistent form of the penalty method, e.g. a form that complies with the norm and inner product of the functional space where the weak formulation is mathematically posed. It is shown that well-known and broadly implemented modelling techniques in the finite element method such as “large mass” and “large spring” techniques arise as limiting cases of this penalty formulation.

Sapountzakis and Dourakopoulos study the nonlinear dynamic analysis of beams of arbitrary doubly symmetric cross section using the boundary element method. The beam is able to undergo moderate large displacements under general boundary conditions, taking into account the effects of shear deformation and rotary inertia. The beam is subjected to the combined action of arbitrarily distributed or

concentrated transverse loading and bending moments in both directions as well as to axial loading. To account for shear deformations, the concept of shear deformation coefficients is used. Five boundary value problems are formulated and solved using the Analog Equation Method. Application of the boundary element technique yields a nonlinear coupled system of equations of motion. The evaluation of the shear deformation coefficients is accomplished from the aforementioned stress functions using only boundary integration.

The chapter of Papachristidis et al. presents the fiber method for the inelastic analysis of frame structures when subjected to high shear. Initially the fiber approach is presented within its standard, purely bending, formulation and it is then expanded to the case of high shear deformations. The element formulation follows the assumptions of the Timoshenko beam theory, while two alternative formulations, a coupled and a decoupled are presented. The numerical examples confirm the accuracy and the computational efficiency of the element formulation under monotonic, cyclic and dynamic/seismic loading.

A simplified procedure to estimate base sliding of concrete gravity dams induced by an earthquake is proposed in the chapter of Basili and Nuti. A simple mechanical model is developed in order to take into account the sources that primarily influence the seismic response of such structures. The dam is modelled as an elastic-linear single-degree-of-freedom-system. Different parameters are considered in the analysis such as the dam height, foundation rock parameters, water level, seismic intensity. As a result, a simplified methodology is developed to evaluate base residual displacement, given the dam geometry, the response spectrum of the seismic input, and the soil characteristics. The procedure permits to assess the seismic safety of the dam with respect to base sliding, as well as the water level reduction that is necessary to render the dam safe.

Papazafeiropoulos et al. provided a literature review and results from numerical simulations on the dynamic interaction of concrete dams with retained water and underlying soil. Initially, analytical closed-form solutions that have been widely used for the calculation of dam distress are outlined. Subsequently, the numerical methods based on the finite element method, which is unavoidably used for complicated geometries of the reservoir and/or the dam, are reviewed. Numerical results are presented illustrating the impact of various key parameters on the distress and the response of concrete dams considering the dam-foundation interaction.

Motivated by the earthquake response of industrial pressure vessels, Karamanos et al. investigate the externally-induced sloshing in spherical liquid containers. Considering modal analysis and an appropriate decomposition of the container-fluid motion, the sloshing frequencies and the corresponding sloshing (or convective) masses are calculated, leading to a simple and efficient method for predicting the dynamic behavior of spherical liquid containers. It is also shown that considering only the first sloshing mass is adequate to represent the dynamic behavior of the spherical liquid container within a good level of accuracy.

Jha et al. introduce a bilevel model for developing an optimal Maintenance Repair and Rehabilitation (MR&R) plan for large-scale highway infrastructure elements, such as pavements and bridges, following a seismic event. The maintenance

and upkeep of all infrastructure components is crucial for mobility, driver safety and guidance, and the overall efficient functioning of a highway system. Typically, a field inspection of such elements is carried out at fixed time intervals to determine their condition, which is then used to develop optimal MR&R plan over a given planning horizon.

Frangopol and Akiyama present a seismic analysis methodology for corroded reinforced concrete (RC) bridges. The proposed method is applied to lifetime seismic reliability analysis of corroded RC bridge piers, and the relationship between steel corrosion and seismic reliability is presented. It is shown that the analytical results are in good agreement with the experimental results regardless of the amount of steel corrosion. Moreover, after the occurrence of crack corrosion, the seismic reliability of the pier is significantly reduced.

Life cycle cost assessment of structural systems refers to an evaluation procedure where all costs arising from owing, operating, maintaining and ultimately disposing are considered. Life cycle cost assessment is considered as a significant assessment tool in the field of the seismic behaviour of structures. Therefore, in the chapter by Mitropoulou et al. two test cases are examined and useful conclusions are drawn regarding the behaviour factor q of EC8 and the incident angle that a ground motion is applied on a multi-storey RC building.

Bal et al. examine vulnerability assessment procedures that include code-based detailed analysis methods together with preliminary assessment techniques in order to identify the safety levels of buildings. Their chapter examines the effect of four essential structural parameters on the seismic behaviour of existing RC structures. Parametric studies are carried out on real buildings extracted from the Turkish building stock, one of which was totally collapsed in 1999 Kocaeli earthquake. Comparisons are made in terms of shear strength, energy dissipation capability and ductility. The mean values of the drop in the performance are computed and factors are suggested to be utilized in preliminary assessment techniques, such as the recently proposed P25 method that is shortly summarized in the chapter.

The aforementioned collection of chapters provides an overview of the present thinking and state-of-the-art developments on the computational techniques in the framework of structural dynamics and earthquake engineering. The book is targeted primarily to researchers, postgraduate students and engineers working in the field. It is hoped that this collection of chapters in a single book will be a useful tool for both researchers and practicing engineers.

The book editors would like to express their deep gratitude to all authors for the time and effort they devoted to this volume. Furthermore, we would like to thank the personnel of Springer Publishers for their kind cooperation and support for the publication of this book.

Athens
June 2010

Manolis Papadrakakis
Michalis Fragiadakis
Nikos D. Lagaros

Contents

Seismic Response of RC Framed Buildings Designed According to Eurocodes

Juan Carlos Vielma, Alex Barbat, and Sergio Oller

Abstract In order to ensure that a structure does not collapse when subjected to the action of strong ground motions, modern codes include prescriptions in order to guarantee the ductile behavior of the elements and of the whole structure. Obviously, it would be of special importance for the designer to know during the design process the extent of damage that the structure will suffer under the seismic action specified by the design spectrum and also the probability of occurrence of different states of behaviour. The incremental nonlinear static analysis procedure used in this paper allows formulating a new, simplified, seismic damage index and damage thresholds associated with five limit states. The seismic behavior of a set of regular reinforced concrete buildings designed according to the EC-2/EC-8 prescriptions for a high seismic hazard level is then studied using the proposed damage index and damage states. Fragility curves and damage probability matrices corresponding to the performance point are calculated for the studied buildings. The obtained results show that the collapse damage state is not reached in the buildings designed according the prescriptions of EC-2/EC-8 and also that the damage does not exceed the irreparable damage limit state.

Keywords Non-linear analysis · Ductility · Overstrength · Objective damage index · Seismic safety

1 Introduction

The main objective of the seismic design is to obtain structures capable to sustain a stable response under strong ground motions. Some of the aspects of the current seismic analysis procedures allow adapting the non-linear features into an

J.C. Vielma (✉)
Lisandro Alvarado University, Decanato de Ingeniería Civil, Av. La Salle, Barquisimeto, Venezuela
e-mail: jcvielma@ucla.edu.ve

A. Barbat and S. Oller
Technical University of Catalonia, c. Gran Capitán s/n 08034, Barcelona, Spain
e-mail: alex.barbat@upc.edu; sergio.oller@upc.edu

M. Papadrakakis et al. (eds.), *Computational Methods in Earthquake Engineering*, Computational Methods in Applied Sciences 21, DOI 10.1007/978-94-007-0053-6_9,

equivalent elastic analysis and, obviously, the formulation of these procedures is essential in assuring a satisfactory earthquake resistant design. The advances in the field of nonlinear structural analysis and the development of improved computational tools enabled to apply more realistic analysis procedures to new and existent buildings, taking into account the main features of their seismic non-linear behaviour, like constitutive nonlinearities (plasticity and damage) and geometrical nonlinearities (large deformations and displacements). Non linear analysis procedures have been used in previous studies to assess the seismic design of buildings designed according to specific design codes [1–3]. The static incremental non-linear analysis (pushover analysis) can be performed by using a predefined lateral load distribution corresponding to the first mode shape. The dynamic analysis can be applied using a suitable set of records obtained from strong motion databases or from design spectrum-compatible synthesized accelerograms. Recently, Performance-Based Design required the definition of a set of limit states. These limit states are frequently defined by engineering demand parameters, among which the most used are the interstory drift, the global drift and the global structural damage. These parameters define damage thresholds associated with the limit states, which allow calculating fragility curves and the damage probability matrices used in the seismic safety assessment of the buildings. In this work, the seismic safety of regular reinforced concrete framed buildings is studied using both the static and the dynamic nonlinear analysis. The static analysis consisted in using pushover procedure and the dynamic analysis was performed by means of incremental dynamic analysis (IDA). The analyses were performed using the PLCd computer code [4] which allows incorporating the main characteristics of the reinforcement and confinement provided to the cross sections of the structural elements. A set of 16 reinforced concrete framed buildings with plan and elevation regularity was designed according to EC-2 [5] and EC-8 [6]. The results obtained from their non-linear analysis allowed calculating the global ductility, the overstrength and the behaviour factors. The latter were compared with the values prescribed by the EC-8. The global performance of the buildings was evaluated using an objective damage index based on the capacity curve. Finally, with the damage thresholds obtained from non-linear analysis, fragility curves and damage probability matrices were computed.

2 Seismic Response Parameters

Among the seismic response parameters studied in past works, global ductility, overstrength and behaviour factor are the most important; they can be calculated by applying deterministic procedures based the non-linear response of the structures subjected to static or dynamic loads. Although it is difficult to find a method to obtain the global yield and the ultimate displacements [7], a simplified procedure is applied in this work. The non-linear static response obtained via finite element techniques is used to generate the idealized bilinear capacity curve shape shown in Fig. 1, which has a secant segment from the origin to a point that corresponds to

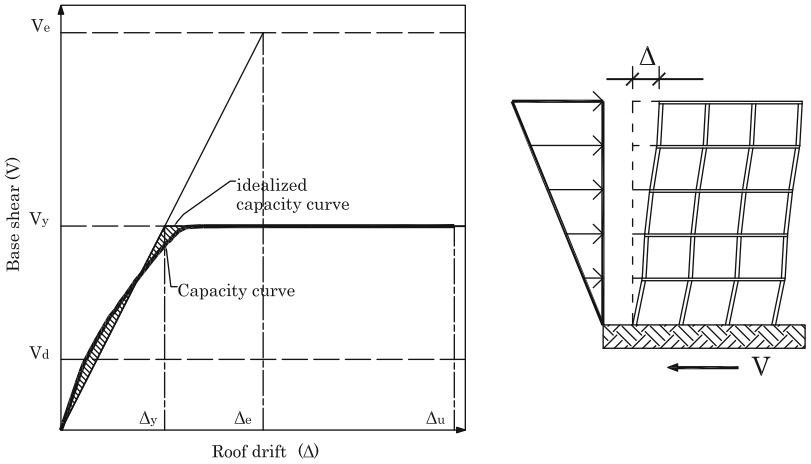

Fig. 1 Scheme for determining displacement ductility and overstrength

a 75% of the maximum base shear [8, 9]. The second segment, which represents the branch of plastic behaviour, was obtained by finding the intersection of the aforementioned segment with another, horizontal segment which corresponds to the maximum base shear. The use this compensation procedure guarantees that the energies dissipated by the ideal system and by the modelled one, are equal (see Fig. 1).

For a simplified non-linear analysis, there are two variables that characterize the quality of the seismic response of buildings. The first is the global ductility μ, defined as

$$\mu = \frac{\Delta_u}{\Delta_y} \tag{1}$$

and calculated based on the values of the yield drift, Δ_y, and of the ultimate drift, Δ_u, which are represented in the idealized capacity curve shown in Fig. 1.

The second variable is the overstrength R_R of the building, which is defined as the ratio of the yielding base shear, V_y to the design base shear, V_d (see Fig. 1)

$$R_R = \frac{V_y}{V_d} \tag{2}$$

3 Local and Objective Damage Index

A local damage index is calculated using the finite element program PLCd with a constitutive damage and plasticity model that enables correlation of damage with lateral displacements [10, 11]

$$D = 1 - \frac{\| P^{in} \|}{\| P_0^{in} \|} \tag{3}$$

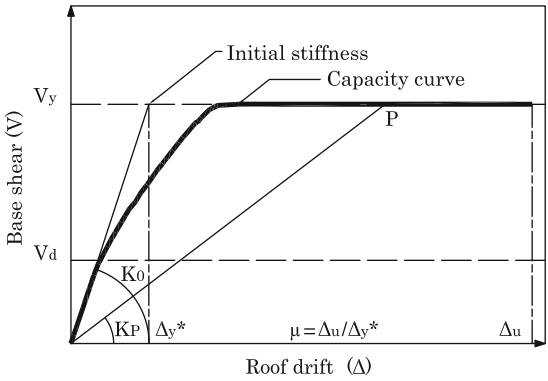

Fig. 2 Parameters for determination of the objective damage-index

where $\|P^{in}\|$ and $\|P_0^{in}\|$ are the norm of current and elastic values of the internal forces vectors, respectively. Initially, the material remains elastic and $D = 0$, but when all the energy of the material has been dissipated $\|P^{in}\| \to 0$ and $D = 1$.

It is important to know the level of damage reached by a structure for a certain demand. This is possible if the damage index is normalized with respect to the maximum damage which can occur in the structure [12]. This objective damage index $0 \leq D_{obj}^{P} \leq 1$ achieved by a structure at any point P is defined as

$$D_{obj}^{P} = \frac{D_P}{D_C} = D_P \frac{\mu}{1-\mu} = \frac{\left(1 - \frac{K_P}{K_0}\right)\mu}{1-\mu} \tag{4}$$

For example, for the point P, which might be the performance point resulting from the intersection between inelastic demand spectrum and the capacity curve (obtained from pu-shover analysis), it corresponds a stiffness K_P. Other parameters are the initial stiffness K_0 and the displacement ductility μ, calculated using the yield displacement Δ_y^* which corresponds to the intersection of the initial stiffness with the maximum shear value (see Fig. 2).

4 Non-linear Response

Non-linear incremental static and dynamic analysis are performed using PLCd finite element code [4,13,14]. PLCd is a finite element code that works with two and three-dimensional solid geometries as well as with prismatic, reduced to one-dimensional members. It provides a solution combining both numerical precision and reasonable computational costs [15,16] and it can deal with kinematics and material nonlinearities. It uses various 3-D constitutive laws to predict the material behaviour (elastic, visco-elastic, damage, damage-plasticity, etc. [17]) with different yield surfaces to control their evolution (Von-Mises, Mohr-Coulomb, improved Mohr-Coulomb, Drucker-Prager, etc. [18]). Newmark's method [10] is used to perform the dynamic analysis. A more detailed description of the code can be found in Mata *et al.*

[15, 16]. The main numerical features included in the code to deal with composite materials are: (1) Classical and serial/parallel mixing theory is used to describe the behaviour of composite components [19]. (2) The Anisotropy Mapped Space Theory enables the code to consider materials with a high level of anisotropy, without the associated numerical problems [20]. (3) The Fiber-matrix debonding, which reduces the composite strength due to the failure of the reinforced-matrix interface, is also considered [21].

Experimental evidence shows that inelasticity in beam elements can be formulated in terms of cross-sectional quantities [22] and, therefore, the beam's behaviour can be described by means of concentrated models, sometimes called plastic hinge models, which localize all the inelastic behaviour at the ends of the beam by means of ad-hoc force-displacement or moment-curvature relationships [23, 24]. But, in the formulation used in this computer program, the procedure consists of obtaining the constitutive relationship at cross-sectional level by integrating on a selected number of points corresponding to the fibers directed along the beam's axis [25]. Thus, the general nonlinear constitutive behaviour is included in the geometrically exact nonlinear kinematics formulation for beams proposed by Simo [26], considering an intermediate curved reference configuration between the straight reference beam and the current configuration. The displacement based method is used for solving the resulting nonlinear problem. Plane cross sections remain plane after the deformation of the structure; therefore, no cross sectional warping is considered, avoiding including additional warping variables in the formulation or iterative procedures to obtain corrected cross sectional strain fields. Thermodynamically consistent constitutive laws are used in describing the material behaviour for these beam elements, which allows obtaining a more rational estimation of the energy dissipated by the structures. The simple mixing rule for composition of the materials is also considered in modelling materials for these elements, which are composed by several simple components. Special attention is paid to obtain the structural damage index capable of describing the load carrying capacity of the structure.

According to the Mixing Theory, in a structural element coexist N different components, all the components undergo same strain; therefore, strain compatibility is forced among the material components. Free energy density and dissipation of the composite are obtained as the weighted sum of the free energy densities and dissipation of the components, respectively. Weighting factors K_q are the participation volumetric fraction of each compounding substance, $K_q = \frac{Vq}{V}$, which are obtained as the quotient between the q-th component volume, V_q, and the total volume, V [13–16].

Discretization of frames was performed with finite elements whose lengths vary depending on the column and beam zones with special confinement requirements. These zones are located near the nodes where the maximum seismic demand is expected, and are designed according to the general dimensions of the structural elements, the diameters of the longitudinal steel, the spans length and the storey heights. Frame elements are discretized into equal thickness layers with different composite materials, characterized by their longitudinal and transversal reinforcement ratio (see Fig. 3). Transverse reinforcement benefits are included by

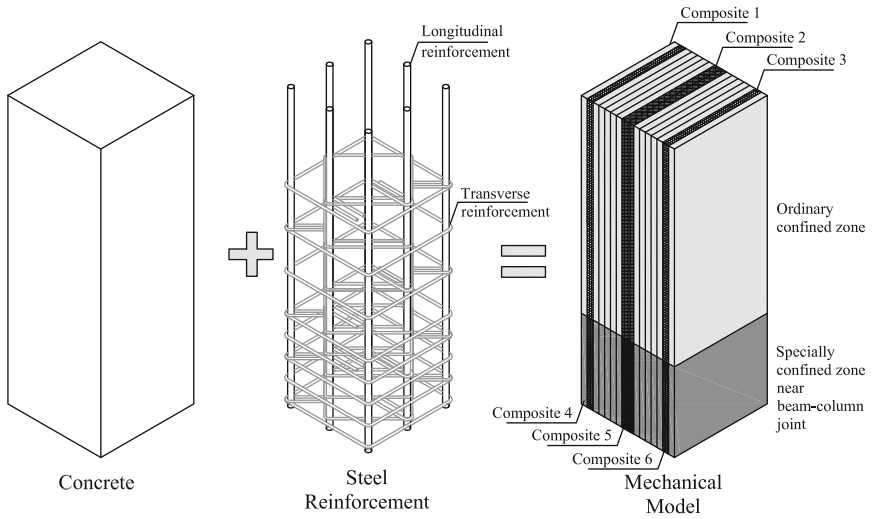

Fig. 3 Discretization of the RC frame's elements

means of the procedure proposed by Mander *et al.* [27]. This procedure consists in improving the compressive strength of the concrete depending on the characteristics of the longitudinal and transversal reinforcement.

5 Design of Buildings

A set of regular reinforced concrete moment-resisting framed buildings (MRFB) designed according to EC-2 and EC-8, characterized by a variable number of storeys (3, 6, 9 and 12) and spans (3, 4, 5 and 6) were selected, in order to cover the low and medium vibration period ranges and also to take into consideration the structural redundancy. Inner and outer frames are defined for each building structure according to the corresponding load ratio (seismic load/gravity load).

The frame members are analyzed designed and detailed following the EC-2 and EC-8 prescriptions for high ductility class (behaviour factor of 5.85). The seismic demand is established for the soil type B (stiff soil) and for a peak ground acceleration of 0.3 g. The geometric characteristics of the typical frames are given in Fig. 4.

5.1 Non-linear Static Analysis

To evaluate the inelastic response of the four structures, pushover analyses were performed applying a set of lateral forces corresponding to seismic actions of the first vibration mode. The lateral forces are gradually increased starting from

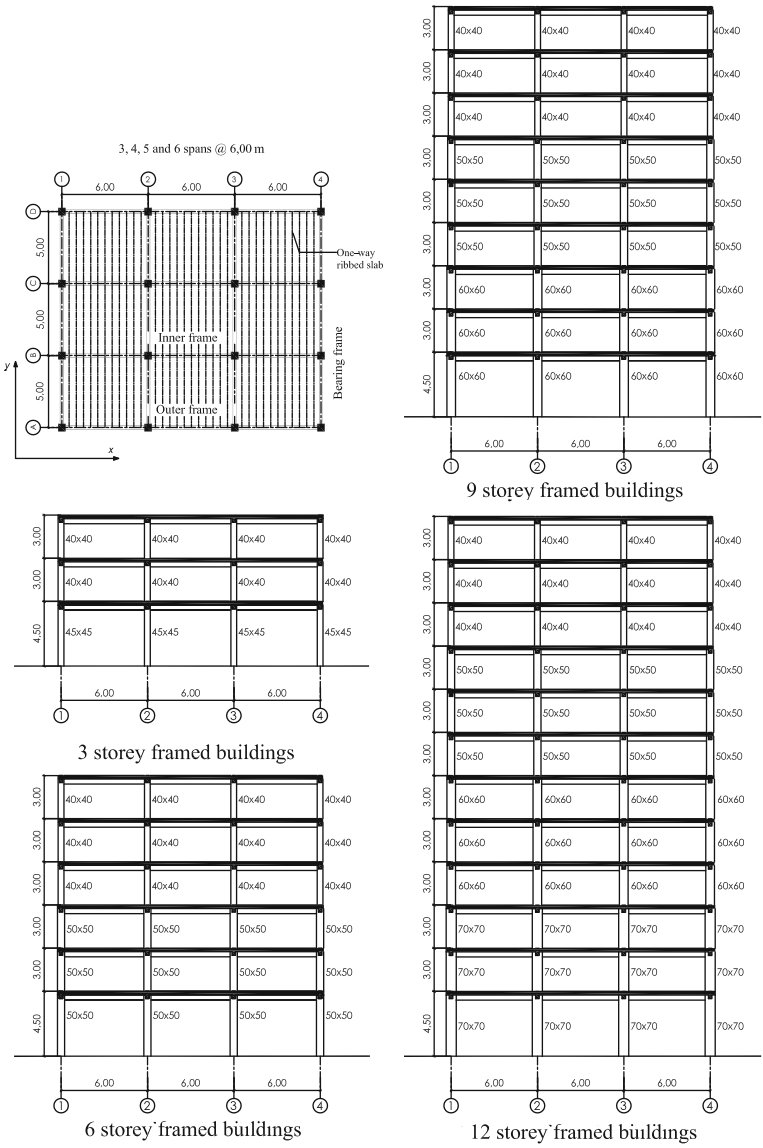

Fig. 4 Plan and elevation view of the framed buildings

zero, passing through the value which induces the transition from elastic to plastic behaviour and, finally, reaching the value which corresponds to the ultimate drift (*i.e.* the point at which the structure can no longer sustain any additional load and collapses). Before the structure is subjected to the lateral loads simulating seismic action, it is first subjected to the action of gravity loads, in agreement with the combinations applied in the elastic analysis. The method applied does not allow for evaluation of torsional effects, being the used model a 2D one.

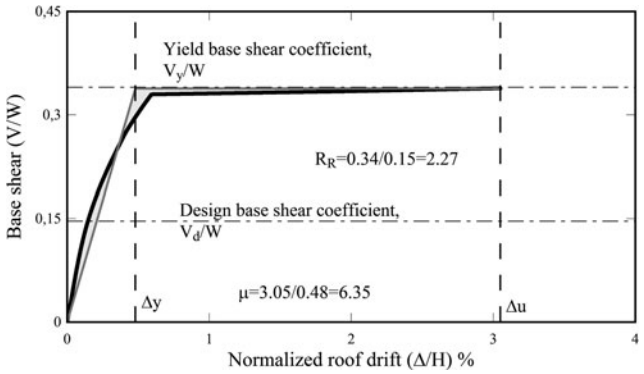

Fig. 5 Typical idealized capacity curve of the studied buildings

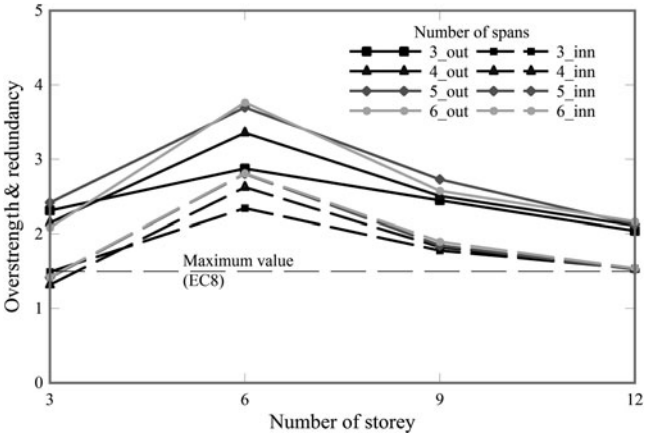

Fig. 6 Overstrength and redundancy vs. the number of storeys of the outer and inner frames

Based on the idealized bilinear curve in Fig. 5, a global ductility of 6.35 is obtained, a higher value than that considered in the EC-8 seismic design code, which is 5.85. From Fig. 5, overstrength is also calculated, obtaining a value of 2.27. This means that the moment resisting buildings designed according to the EC-2 and EC-8 have a ductile response to seismic forces, as well as an adequate overstrength.

Figure 6 shows the computed values of the overstrength for the outer and inner frames of the studied buildings, plotted in function of the number of storeys. The results demonstrate clearly that the influence of the number of spans, equivalent to consider different numbers of resistant lines, is very low, except for the case of the 6 storey buildings. For the other buildings, the overstrength values are closer to each other. It can be also seen that the computed values of the combined overstrength factors are greater than the value which the EC-8 prescribes for the design of ductile framed buildings.

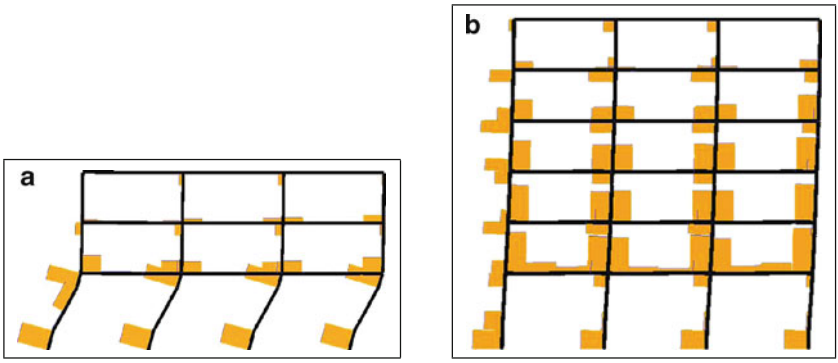

Fig. 7 Distribution of local damage-index at collapse displacement

The local damage index is calculated using Eq. (3) and the results are shown in Fig. 7 for the inner frames of the 3 and 6 storey buildings, for the collapse displacement. In this figure, each rectangle represents the magnitude of the damage reached by the element. It is important to observe that for the low rise buildings (N = 3) the maximum values of the damage corresponds to the elements located at both ends of the first storey columns; this damage concentration corresponds to a soft-storey mechanism. Instead, high rise buildings (N = 6, 9 and 12) show their maximum damage values at low level beams ends, according to the desired objective of the conceptual design which is to produce structures with weak beams and strong columns.

Figure 8 show the interstory drifts at collapse. It is important to note the difference among the interstory values for the three levels building, which reaches very high value at the ground level (Fig. 8a). This feature is a consequence of the soft-story mechanism characterized by the concentration of the damage in the columns of this story. The interstory drifts of the 6, 9 and 12 levels buildings reach values near 4%, without a predominant value in a specific story. From the non-linear static analysis, the objective damage index is computed using Eq. (3).

Figure 9 shows the evolution of the objective damage index respecting the normalized roof drift, computed for all the frames of the 3 storey building. The curves are similar to those obtained for the frames of the same number of stories.

5.2 Non-linear Dynamic Analysis

In order to evaluate the dynamic response of the buildings, IDA (Incremental Dynamic Analysis) procedure was applied [28], which consists in performing time-history analyses for actual ground motion accelerograms or for artificially

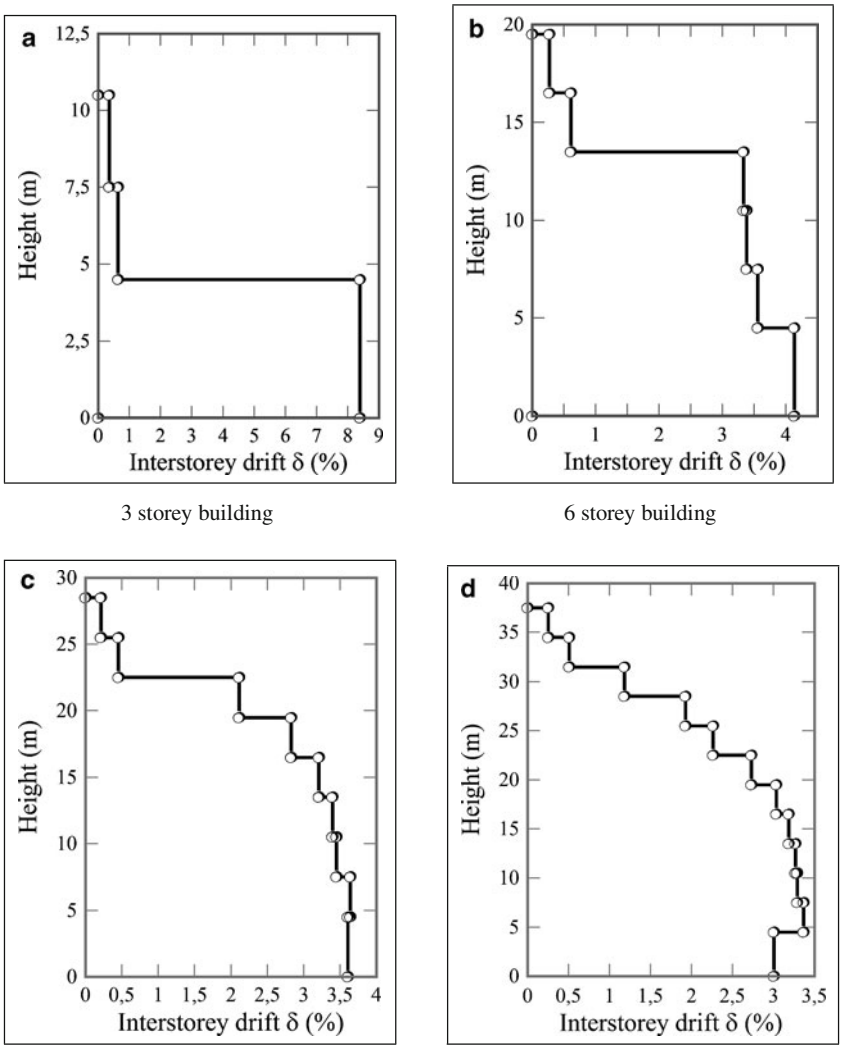

Fig. 8 Interstory drifts at the collapse

synthesized accelerograms scaled in such a way to induce increasing levels of inelasticity in each new analysis. A set of six artificial accelerograms, compatible with the soil type B of EC-8 design spectrum, were generated. Figure 10 shows the elastic design spectrum and the 5% damping response spectra computed from the set of artificial accelerograms.

Peak accelerations equal to the basic design acceleration is assumed in the analysis. From this value, the record is scaled until a plastic response is reached by the structure; this procedure continues until achieving the collapse displacement.

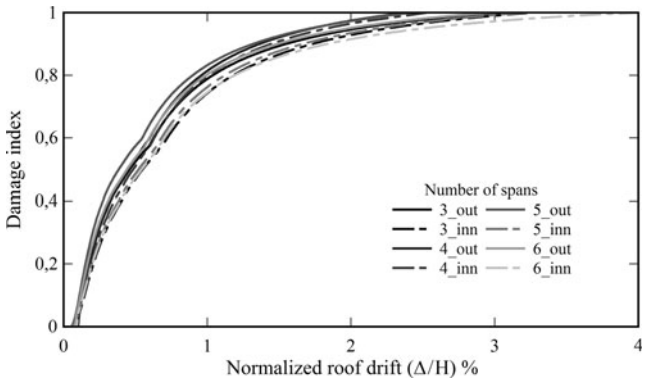

Fig. 9 Evolution of the damage index of the 3 storey inner and outer frames

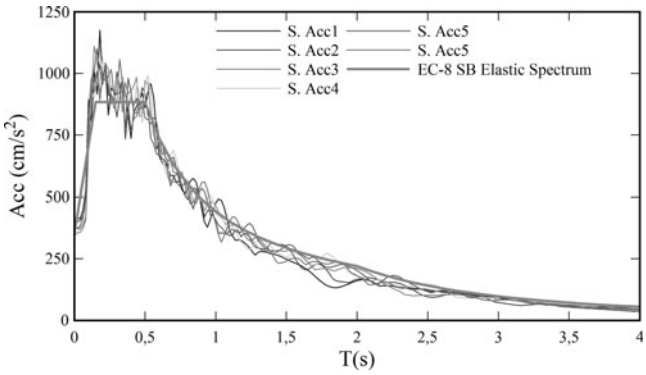

Fig. 10 EC-8 soil type B, elastic design spectrum and response spectra

For each value of scaled acceleration, a maximum value of the structural response is calculated. The IDA curves are obtained by plotting a maximum characteristic of the severity of the earthquake in function of a maximum value of the structural response. In this case, we represented the spectral acceleration for a 5% damping ratio against the roof drift. The collapse is reached when the capacity of the structure drops [29–31]. A usual criterion is to consider that collapse occurs when the slope of the curve is less than the 20% of the elastic slope [28, 31, 32]. Figure 11 show the IDA curves computed for the 3-spans outer frames of the 3, 6, 9 and 12 storey buildings. Note that the collapse points of the frames are closer to the values obtained from the static pushover analysis, validating the collapse threshold values.

Table 1 summarizes the computed average values of the collapse points for all the studied cases, computed by means of the dynamic analysis.

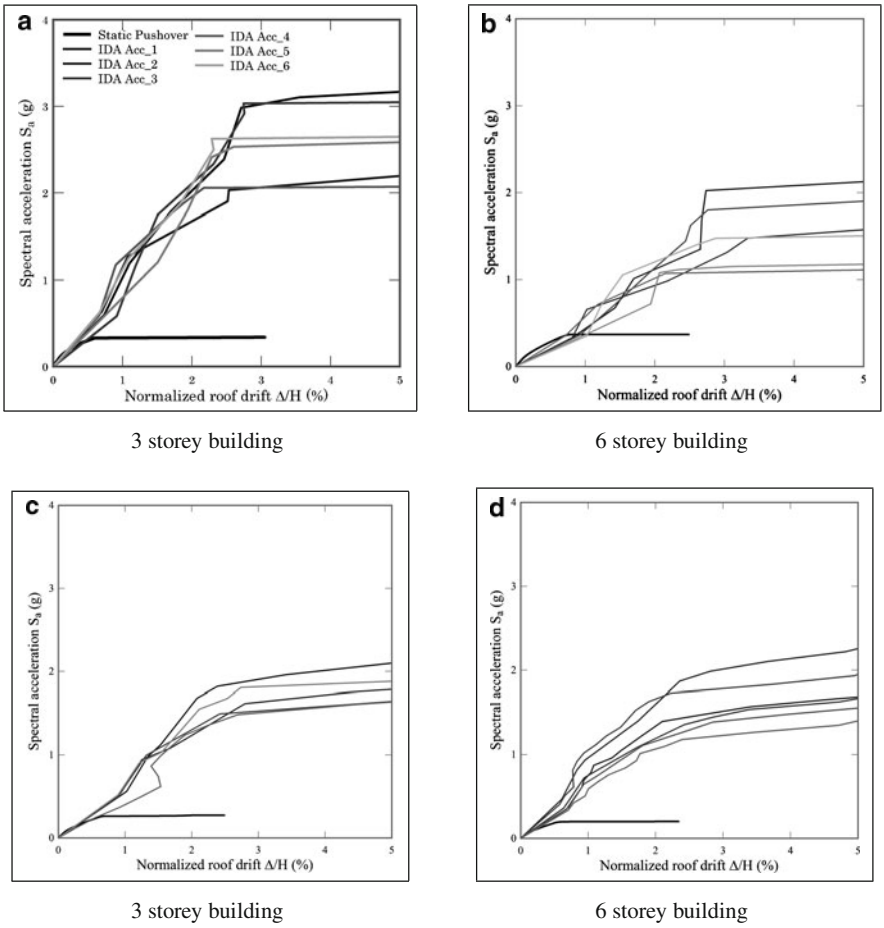

3 storey building

6 storey building

3 storey building

6 storey building

Fig. 11 IDA curves of the outer frames of the buildings

Table 1 Normalized roof displacement (%) at the collapse of the structures

Number of storeys	Static analysis	Dynamic analysis (average)
3	2.51	2.51
6	2.63	2.63
9	2.48	2.62
12	2.35	2.39

The dynamic analysis is useful to assess the collapse point of the buildings. For the behaviour factors q, the following equation has been proposed [2]:

$$q = \frac{a_{g\,(Collapse)}}{a_{g\,(Design-yield)}} \tag{5}$$

Table 2 Computed behaviour factors of the buildings

Number of storeys	$q_{equation}$	q_{code}	$\frac{q_{equation}}{q_{code}}$
3	17.40	5.85	2.97
6	10.79	5.85	1.84
9	15.07	5.85	2.57
12	15.12	5.85	2.58

where $a_{g(Collapse)}$ and $a_{g(Design-yield)}$ are the collapse and the yield design peak ground acceleration, respectively. The former is obtained from the IDA curves and the latter is calculated from the elastic analysis of the building. Average values of the computed behaviour factor q of the studied buildings are show in Table 2; these values correspond to the dynamic response obtained for the set of six synthesized accelerograms, and are compared with behaviour factors prescribed by the design codes.

The computed behaviour factors show that seismic design performed by using the EC-2 and EC-8 leads to structures with satisfactory lateral capacity, when they are subjected to strong motions, regardless of the building height. The relationship between the calculated and the prescribed behaviour factors is close to three for the case of low rise buildings.

6 Seismic Safety of the Buildings

Studying the seismic safety of the buildings designed according to the Eurocodes requires to define and compute the engineering demand measure (EDM). It is usual to select the interstory and the global drifts as EDM; in this article, the latter was selected. In order to assess the seismic safety, the global drifts correspond to the performance point have been determined as described in the following.

6.1 Determination of the Performance Point

In order to evaluate the non-linear behaviour of the buildings, the performance points, which represent the maximum drift of an equivalent single degree of freedom induced by the seismic demand, were calculated. These points have been determined by means of the N2 procedure [33] which requires transforming the capacity curve into a capacity spectrum expressed in terms of the spectral displacement, S_d, and of the spectral acceleration, S_a. The former is obtained by means of the equation

$$S_d = \frac{\delta_c}{MPF} \tag{6}$$

where δ_c is the roof displacement. The term MPF term is the modal participation factor calculated from the response in the first mode of vibration.

$$MPF = \frac{\sum_{i=1}^{n} m_i \phi_{1,i}}{\sum_{i=1}^{n} m_i \phi_{1,i}^2} \tag{7}$$

Spectral acceleration S_a is calculated by means of:

$$S_a = \frac{\frac{V}{W}}{\alpha} \tag{8}$$

where V is the base shear, W is the seismic weight and α is a coefficient obtained as

$$\alpha = \frac{\left(\sum_{i=1}^{n} m_i \phi_{1,i}\right)^2}{\sum_{i=1}^{n} m_i \phi_{1,i}^2} \tag{9}$$

Figure 12 shows a typical capacity spectrum crossed with the corresponding elastic demand spectrum. Idealized bilinear shape of the capacity spectra is also shown.

The values of the spectral displacements corresponding to the performance point are shown in Table 3. An important feature which influences on the non linear

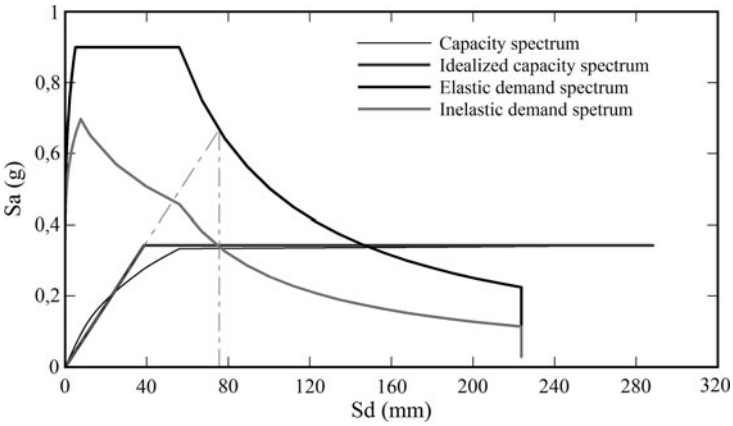

Fig. 12 Determination of the performance point according to N2 procedure

Table 3 Roof drift of performance points of the studied buildings

	Normalized roof drift			Ratio	
Number of stories	Performance point (%)	Static analysis	Dynamic analysis (average)	Static analysis	Dynamic analysis (average)
3	0.80	3.02	2.51	0.26	0.32
6	0.51	2.48	2.63	0.20	0.19
9	0.39	2.48	2.62	0.16	0.15
12	0.21	2.34	2.39	0.09	0.09

response of the buildings is the ratio between the performance point displacement and the collapse displacement. This ratio indicates whether the behaviour of a structure is ductile or fragile. The lower values correspond to the 12 storey buildings, which have a weak-beam strong column failure mechanism.

6.2 Fragility Curves and Damage Probability Matrices

The damage thresholds are determined using the VISION 2000 procedure [34], in which they are expressed in function of interstory drifts. In this article, five damage states thresholds are defined from both the interstory drift curve and the capacity curve [35]. For the slight damage state, the roof drift corresponding to the first plastic hinge is considered. The moderate damage state corresponds to the roof drift for which an interstory drift of 1% is reached in almost all the storeys of the structure. The repairable damage state is defined by an interstory drift of 2%. The severe damage state is identified by a roof drift producing a 2,5% of interstory drift at each level of the structure. Finally, the total damage state (collapse) corresponds to the ultimate roof displacement obtained from the capacity curve. Mean values and standard deviation were computed from the non linear response of the buildings with the same geometry and structural type, varying the number of spans from 3 to 6 [36].

Fragility curves are obtained by using the spectral displacements determined for the damage thresholds and considering a lognormal probability density function for the spectral displacements which define the damage states [37–40]

$$F(S_d) = \frac{1}{\beta_{ds} S_d \sqrt[n]{2\pi}} \exp\left[-\frac{1}{2}\left(\frac{1}{\beta_{ds}} \ln \frac{S_d}{\bar{S}_{d,ds}}\right)^2\right] \tag{10}$$

where $\bar{S}_{d,ds}$ is the mean value of spectral displacement for which the building reaches damage state threshold d_s and β_{ds} is the standard deviation of the natural logarithm of spectral displacement for damage state d_s. The conditional probability $P(S_d)$ of reaching or exceeding a particular damage state d_s, given the spectral displacement S_d, is defined as

$$P(S_d) = \int_0^S F(S_d) dS_d \tag{11}$$

Figure 13 show the fragility curves calculated for the four different heights of buildings considered in the analysis.

Figure 14 shows the damage probability matrices calculated for the performance point achieved for all the studied cases. It is important to note that for frames of the same building, probabilities vary according to the load ratio (seismic load/gravity load).

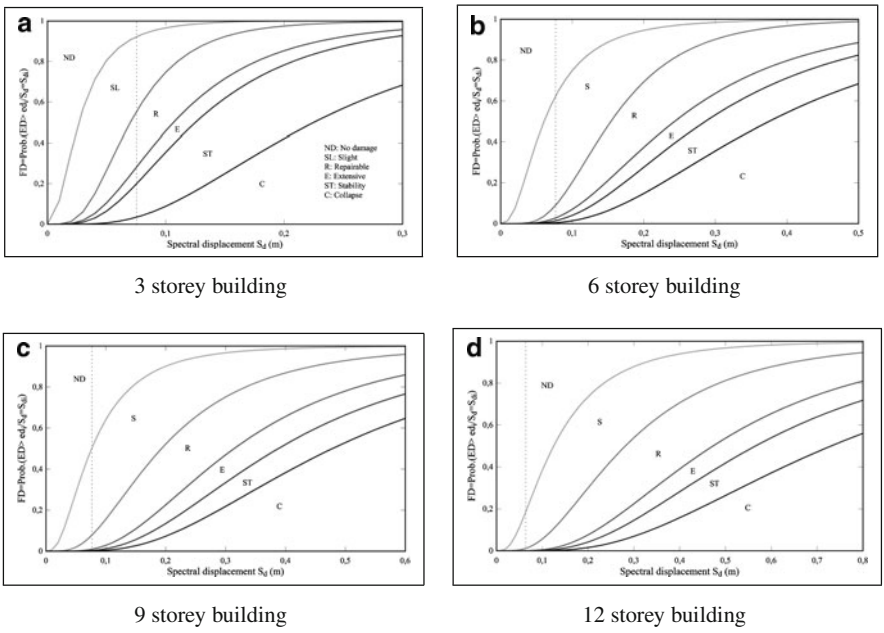

3 storey building

6 storey building

9 storey building

12 storey building

Fig. 13 Fragility curves of the buildings

Another important feature is the increasing values of the probabilities that low rise buildings reach higher damage states; the collapse of these buildings is associated with the soft-storey mechanism, as discussed in previous sections. For example, in the case of the inner frames of the three level building, the probability to reach the collapse is four times higher than in the case of the outer frame of the same building. In contrast, 6, 9 and 12 storey buildings show very low probabilities to reach higher damage states, regardless of the load ratio and of the span number. For these buildings, the predominant damage states are *non-damage* and *slight damage*.

Figure 15 shows the values of the damage index for the performance point of the different frames. These values were obtained using Eq. (3). First of all, it is possible to observe that low rise buildings (three levels) reach higher values of the damage index than the other buildings, as a consequence of the failure mechanism which occurs for this kind of buildings (soft storey mechanism). In contrast, the 12 level buildings exhibits damage indices about 0.3 and 0.35 for the inner and outer frames respectively, values that are consistent with the failure mechanism (strong columns-weak beams). Finally it is important to observe that the values of the damage index obtained for the outer frames are lower than those corresponding to the inner ones, indicating that the damage index depends on the load type ratio [41].

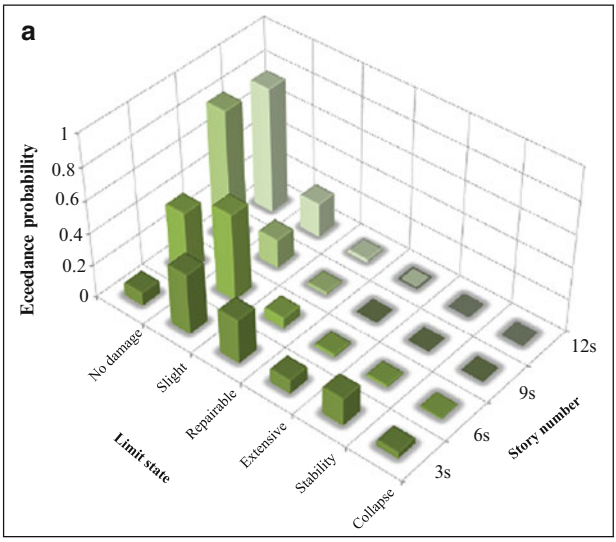

Outer frames

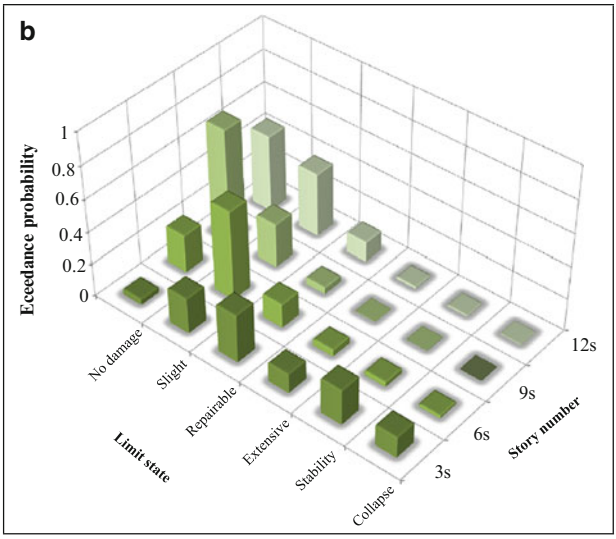

Inner frames

Fig. 14 Damage probability matrices of 3, 6, 9 and 12 storey buildings

7 Concluding Remarks

The proposed objective damage index predicts adequately the state of damage that is achieved by the frames for a specific seismic demand value (displacement of the performance point).

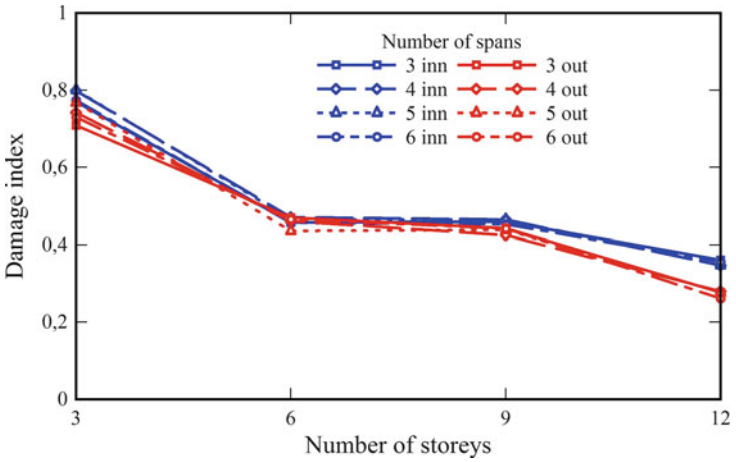

Fig. 15 Damage index computed for the performance point of the 3 storey building frames

The Incremental Dynamic Analysis is useful in order to assess the collapse threshold of the frames. Dynamic results confirm the values obtained from pushover analysis. The dynamic analysis is also suitably to evaluate the behaviour factor q.

In general, the reinforced concrete framed buildings designed according to the Eurocodes for a high ductility class show adequate ductility behaviour, as it is evidenced by the global ductility values and the ratio between the performance point and the ultimate displacement. They also exhibit adequate values of overstrength, which are greater than the code prescribed value (overstrength $= 1.5$). Behaviour factors computed from dynamic analysis are also adequate and reach twice the code values. No influence of the structural redundancy was detected in the procedure applied to evaluate such factors.

The nonlinear response of the buildings depends on the load ratio between the seismic and gravity loads; the inner frames which are designed for lower load ratios have lower overstrength values. Consequently, the seismic safety of the different frames is influenced by this ratio.

The local damage distribution when the buildings reach the collapse threshold, show that low rise buildings (3 storey) have a failure mechanism associated with the formation of the soft storey mechanism. Medium height buildings (6, 9 and 12 storey) exhibit a failure mechanism associated with the conceptual design objective of designing structures with weak-beam and strong column. The interstory drifts of the low rise building show that the damage is concentrated into the ground level, where the interstory drift reached a value greater than 8%. Mid-rise buildings show more uniform values of the interstory drifts and their values are lower than 4%. These results evidenced that the low-rise building collapse corresponds to soft-story mechanism.

References

1. Mwafi AM, Elnashai A (2002) Overstrength and force reduction factors of multistory reinforced-concrete buildings. Struct Des Tall Buil 11:329–351
2. Mwafi AM, Elnashai A (2002) Calibration of force reduction factors of RC buildings. J Earthquake Eng 6(2):239–273
3. Sanchez AM, Plumier L (2008) Parametric study of ductile moment-resisting steel frames: a first step towards Eurocode 8 calibration. Earthquake Eng Struct Dynam 37:1135–1155
4. PLCd (2009) Non-linear thermo mechanic finite element oriented to PhD student education, code developed at CIMNE, Barcelona, Spain
5. Comité Européen de Normalisation (2001) Eurocode 2: Design of concrete structures BS EN 1992, Brussels
6. Comité Européen de Normalisation (2001) Eurocode 8: Design of structures for earthquake resistance EN 2004-1-1, Brussels
7. Priestley MJN, Calvi GM, Kowalsky MJ (2007) Displacement-based seismic design of structures. IUSS Press, Pavia, Italy
8. Park R (1998) State-of-the-art report: ductility evaluation from laboratory and analytical testing. In: Proceedings 9th WCEE. IAEE, Tokyo, Japan
9. Vielma JC, Barbat AH, Oller S (2009) Seismic performance of Waffled-Slab floor buildings. Proc P I Civil Eng Str 16(3):169–182
10. Barbat AH, Oller S, Oñate E, Hanganu A (1997) Viscous damage model for Timoshenko beam structures. Int J Solid Struct 34(30):3953–3976
11. Car E, Oller S, Oñate E (2000) Seismic performance of Waffled-Slab floor buildings. Comput Meth Appl Mech Eng 185(2–4):245–277
12. Vielma JC, Barbat AH, Oller S (2008) An objective seismic damage index for the evaluation of the performance of RC buildings. In: Proceedings 14th WCEE. IAEE, Beijing, China
13. Oller S, Barbat AH (2006) Moment-curvature damage model for bridges subjected to seismic loads. Comput Meth Appl Mech Eng 195:4490–4511
14. Car E, Oller S, Oñate E (2001) A large strain plasticity for anisotropic materials: composite material application. Int J Plast 17(1):1437–1463
15. Mata P, Oller S, Barbat AH (2007) Static analysis of beam structures under nonlinear geometric and constitutive behaviour. Comput Meth Appl Mech Eng 196:4458–4478
16. Mata P, Oller S, Barbat AH (2007) Dynamic analysis of beam structures under nonlinear geometric and constitutive behaviour. Comput Meth Appl Mech Eng 197:857–878
17. Oller S, Oliver J, Oñate E, Lubliner J (1990) Finite element non-linear analysis of concrete structures using a plastic-damage model. Eng Fract Mech 35(1-3):219–231
18. Lubliner J, Oliver J, Oller S, Oñate E (1989) A plastic-damage model for concrete. Int J Solid Struct 25(3):299–326
19. Faleiro J, Oller S, Barbat AH (2008) Plastic-damage seismic model for reinforced concrete frames. Comput Struct 86:581–597
20. Oller S, Car E, Lubliner J (2003) Definition of a general implicit orthotropic yield criterion. Comput Meth Appl Mech Eng 192(7–8):895–912
21. Martinez X, Oller S, Rastellini F, Barbat AH (2008) A numerical procedure simulating RC structures reinforced with FRP using the serial/parallel mixing theory. Comput Struct 86:1604–1618
22. Bayrak O, Sheikh SA (2001) Plastic hinge analysis. J Struct Eng (ASCE) 127:1092–1100
23. Spacone E, El Tawil S (2000) Nonlinear analysis of steel-concrete composite structures: state of the art. J Struct Eng (ASCE) 126:159–168
24. Faleiro J, Oller S, Barbat AH (2010) Plastic-damage analysis of reinforced concrete frames. Eng Computations 27(1):57–83
25. Shao Y, Aval S, Mirmiran A (2005) Fiber-element model for cyclic analysis of concrete-filled fiber reinforced polymer tubes. J Struct Eng (ASCE) 131:292–303
26. Simo JC (1985) A finite strain beam formulation. The three-dimensional dynamic problem Part I. Comput Meth Appl Mech Eng 49:55–70

27. Mander JB, Priestley MJN, Park R (1988) Observed stress-strain behaviour of confined concrete. J Struct Eng (ASCE) 114:1827–1849
28. Vamvatsikos D, Cornell, CA (2002) Incremental dynamic analysis. Earthquake Eng Struct Dynam 31(3):491–514
29. Kunnath, S (2005) Performance-based seismic design and evaluation of buildings structures. In: Chen WF, Lui EM (eds), Earthquake engineering for structural design. CRC, Boca Raton Press
30. Vielma JC, Barbat AH, Oller S (2009) Reserva de resistencia de edificios porticados de concreto armado diseados conforme al ACI-318/IBC-2006. Revista de Ingeniera de la Universidad de Costa Rica 18(1,2):121–131
31. Vielma JC, Barbat AH, Oller S (2010) Seismic safety of low ductility structures used in Spain. Bull Earthquake Eng 8:135–155
32. Han SW, Chopra A (2006) Approximate incremental dynamic analysis using the modal pushover analysis procedure. Earthquake Eng Struct Dynam 35(3):1853–1873
33. Fajfar PA (2000) Nonlinear analysis method for performance based seismic design. Earthquake Spectra 16(3):573–591
34. SEAOC (1995) Vision 2000 report on performance based seismic engineering of buildings. Structural Engineers Association of California, vol I. Sacramento, California
35. Vielma JC, Barbat AH, Oller S (2008) Umbrales de daño para estados lmite de edificios porticados de concreto armado diseados conforme al ACI-318/IBC-2006. Revista Internacional de Desastres Naturales, Accidentes e Infraestructura 8:119–134
36. Vielma JC (2008) Caracterizacin de la respuesta ssmica de edificios de hormign armado mediante la respuesta no lineal, PhD Thesis, Barcelona, Spain
37. Pinto PE, Giannini R, Franchin P (2006) Seismic reliability analysis of structures. IUSS Press, Pavia, Italy
38. Barbat AH, Pujades LG, Lantada N (2008) Seismic damage evaluation in urban areas using the capacity spectrum method: application to Barcelona. Soil Dyn Earthquake Eng 28:851–865
39. Barbat AH, Pujades LG, Lantada N (2006) Performance of buildings under earthquakes in Barcelona, Spain. Comput-Aided Civ Infrastruct Eng 21:573–593
40. Lantada N, Pujades LG, Barbat AH (2009) Vulnerability index and capacity spectrum based methods for urban seismic risk evaluation. A comparison. Nat Hazards 51:501–524
41. Vielma JC, Barbat AH, Oller S (2010) Non-linear structural analysis. Application for evaluating the seismic safety. In: Structural analysis. Nova Science Publishers, New York